

# Time and rate dependent constitutive model coupled with nonlocal damage at finite strains for semi-crystalline polymers

Romain Balieu<sup>a</sup>, Franck Lauro<sup>a</sup>, Bruno Bennani<sup>a</sup>

Tsukatada Mastumoto<sup>b</sup>, Ernesto Mottola<sup>b</sup>

a Univ Lille Nord de France, F-59000 Lille, France

a UVHC, LAMIH, F-59313 Valenciennes, France

a CNRS, UMR 8201, F-59313 Valenciennes, France

b TOYOTA MOTOR EUROPE, Brussels, Belgium

## 1 Introduction

Many constitutive models were developed in the literature to model the complex behaviour of polymer materials. These models can be sorted in two categories: the physical based models where the microstructure of the material is taken into account for representing the macroscopic behaviour [1,2] and the phenomenological based models where the material discontinuities, in the microstructural scale, are homogenised in a representative volume element. In this way, elasto-plastic constitutive models based on the “overstress” concept (VBO) [3] using the unified state variable theory were extended for polymeric materials [4,5]. The addition of mineral fillers in the semi-crystalline matrix increases the cavitation phenomenon. In this case, the viscoelastic-viscoplastic deformation of the material is accompanied by damage in the form of nucleation, growth and coalescence of cavities. Many damage model were developed for polymer application in order to represent this phenomenon [6,7,8,9]. The damage present in this kind of material induces a softening behaviour which leads to the localisation of the strain in a narrow zone of the structure accompanied by numerical solutions depending of the finite element mesh. The nonlocal model where introduced in the literature in this way, in order to overcome the mesh dependency phenomenon [10,11].

In this work, a non-associated viscoelastic-viscoplastic model coupled with nonlocal damage is developed in order to model a mineral filled semi-crystalline polymer used in the automotive industry. The constitutive equations of the model are stated under finite strain framework by using a hypoelastic formulation. The interesting properties of the logarithmic tensor linking the work conjugate pair Cauchy stress and Henky strain are used in the proposed model. In order to obtain a mesh independent solution with the material exhibiting softening, an integral-type nonlocal damage is developed in this work.

## 2 Constitutive model

In the proposed model, the direct relation linking the second order stretching tensor  $\underline{\mathbf{D}}$  and the corotational rate of the Henky strain tensor  $\overset{\circ}{\mathbf{h}}^{\log}$  proposed by Xiao et al. [12] is used, i.e.,

$$\overset{\circ}{\mathbf{h}}^{\log} = \dot{\mathbf{h}} - \underline{\mathbf{\Omega}}^{\log} \mathbf{h} + \mathbf{h} \underline{\mathbf{\Omega}}^{\log} = \underline{\mathbf{D}} \quad (1)$$

where  $\mathbf{h}$  is the Henky strain tensor and  $\underline{\mathbf{\Omega}}^{\log}$  the logarithmic spin tensor defined by

$$\underline{\underline{\Omega}}^{\log} = \underline{\underline{W}} + \sum_{i,j=1,i \neq j}^m \left[ \frac{1 + \left( \frac{b_i}{b_j} \right)}{1 - \left( \frac{b_i}{b_j} \right)} + \frac{2}{\log \left( \frac{b_i}{b_j} \right)} \right] \underline{\underline{P}}_i \underline{\underline{D}} \underline{\underline{P}}_i, \quad (2)$$

where  $b_i = \lambda_i^2$  are the eigenvalues of the left Cauchy-Green deformation tensor  $\underline{\underline{B}}$  and  $\underline{\underline{P}}_i$  are the eigenprojection subordinate to eigenvalues  $\lambda_i > 0$  of the left stretch tensor  $\underline{\underline{V}}$ . The hypoelastic formulation of the viscoelastic-viscoplastic model is used assuming the additive decomposition of the stretching tensor in a viscoelastic  $\underline{\underline{D}}^{ve}$  and a viscoplastic  $\underline{\underline{D}}^{vp}$  part, i.e.,

$$\overset{\circ}{\underline{\underline{\sigma}}}^{\log} = \mathfrak{F}(\underline{\underline{\sigma}}, \underline{\underline{D}}^{ve}) = \mathfrak{F}(\underline{\underline{\sigma}}, \underline{\underline{D}} - \underline{\underline{D}}^{vp}) = \mathfrak{F} \left( \underline{\underline{\sigma}}, \underline{\underline{h}} - \left( \underline{\underline{h}}^{vp} \right)^{\log} \right). \quad (3)$$

By using the corotational integration of a corotational rate of an Eulerian second order tensor  $\underline{\underline{a}}^{\circ \log}$ , i.e.,

$$\int_{\text{corot}} \overset{\circ}{\underline{\underline{a}}}^{\log} = \underline{\underline{a}}, \quad \text{the general form of the constitutive model is given by}$$

$$\underline{\underline{\sigma}} = \mathfrak{F}(\underline{\underline{\sigma}}, \underline{\underline{h}} - \underline{\underline{h}}^{vp}). \quad (4)$$

The linear viscoelastic model of Wierchert (generalised Maxwell model) is used in order to model the strain rate sensitivity on the stiffness of the material. The damaged stress tensor given by the viscoelastic model at time  $t$ , i.e.  $\underline{\underline{\sigma}}(t)$ , resulting of a viscoelastic strain increment at time  $\zeta$  is defined such as

$$\underline{\underline{\sigma}}(t) = (1 - D) \int_{-\infty}^t \left\{ \underline{\underline{L}}_{\infty}^{ve} + \sum_{i=1}^N \underline{\underline{L}}_i^{ve} \exp \left( -\frac{t - \zeta}{\tau_i} \right) \right\} : \frac{d\underline{\underline{h}}^{ve}(\zeta)}{d(\zeta)} d(\zeta), \quad (5)$$

where  $D$  is the isotropic damage variable,  $\tau_i$  are the relaxation times of each Maxwell element,  $\underline{\underline{L}}_{\infty}^{ve}$  and  $\underline{\underline{L}}_i^{ve}$  are the fourth order long term elastic stiffness tensor and the elastic stiffness tensor of the  $i^{\text{th}}$  Hook element included in the  $i^{\text{th}}$  Maxwell element, respectively given by

$$\underline{\underline{L}}_{\infty}^{ve} = 2G_{\infty} \underline{\underline{I}}_d + K_{\infty} \underline{\underline{I}} \otimes \underline{\underline{I}}^2 \quad \text{and} \quad \underline{\underline{L}}_i^{ve} = 2G_i \underline{\underline{I}}_d + K_i \underline{\underline{I}} \otimes \underline{\underline{I}}, \quad (6)$$

where  $G_{\infty}$ ,  $K_{\infty}$ ,  $G_i$ ,  $K_i$  are the long term and instantaneous shear and bulk moduli, respectively.

In order to take the hydrostatic pressure sensitivity of the material into account, the yield surface given by Raghava et al. [13] depending on the second invariant  $J_2$  of the deviatoric stress tensor  $\underline{\underline{S}}$  and on the first invariant  $I_1$  of the stress tensor is used in the constitutive model. This yield surface is defined as follows:

$$f^{vp}(\underline{\underline{\sigma}}, R, D) = \frac{(\eta - 1)I_1(\underline{\underline{\sigma}}) + \sqrt{(\eta - 1)^2 I_1^2(\underline{\underline{\sigma}}) + 12\eta J_2(\underline{\underline{S}})}}{2\eta(1 - D)} - \sigma_t - R(\kappa), \quad (7)$$

where  $\eta$  is the ratio between the tensile and compression yield stress, i.e.  $\sigma_t$  and  $\sigma_c$ , respectively and  $R$  is the isotropic hardening law defined such as

<sup>1</sup>  $\underline{\underline{I}}_d$  is the fourth order deviatoric projection tensor.

<sup>2</sup>  $\underline{\underline{I}}$  is the second order identity tensor.

$$R(\kappa) = Q_1 \kappa \exp(-b_1 \kappa) + Q_2 (1 - \exp(-b_2 \kappa)) + b_3 \kappa^3 + b_4 \kappa^2 + b_5 \kappa, \quad (8)$$

$Q_1, Q_2, b_1, b_2, b_3, b_4$  and  $b_5$  are material parameters. The hardening variable used in Eq. (8) is the equivalent viscoplastic strain, i.e.,

$$\kappa = \sqrt{\frac{2}{3} \underline{\mathbf{h}}^{vp} : \underline{\mathbf{h}}^{vp}}. \quad (9)$$

The deformation of polymeric material is not an isochoric phenomenon. The non-associated plasticity is therefore used in order to represent this volume variation. A second dissipation potential  $F$  (which is different to the yield surface  $f$ ) is also postulated as follows:

$$F(\underline{\boldsymbol{\sigma}}) = \frac{\sqrt{3J_2(\underline{\mathbf{S}}) + \alpha^+ \langle p \rangle^2 + \alpha^- \langle -p \rangle^2}}{1 - D}, \quad (10)$$

where  $\alpha^+$  and  $\alpha^-$  are parameters which define the volume variation for positive and negative hydrostatic pressures, respectively. The symbol  $\langle \bullet \rangle$  is the Macauley bracket, that is, for any scalar  $x$ , given by  $(x + |x|)/2$ . With this formulation, the flow direction of the rate of the viscoplastic strain tensor for positive (dilatation) and negative (compaction) pressures can evolve independently. According to the non-associated flow rule, the viscoplastic strain rate tensor is given by

$$\underline{\dot{\mathbf{h}}}^{vp} = \dot{\lambda} \frac{\delta F}{\delta \underline{\boldsymbol{\sigma}}} = \dot{\lambda} \underline{\mathbf{n}}, \quad (11)$$

where  $\underline{\mathbf{n}}$  is the direction of the viscoplastic flow expressed as

$$\underline{\mathbf{n}} = \frac{1}{g(1 - D)} \left( \frac{3}{2} \underline{\mathbf{S}} + \frac{1}{3} (\alpha^+ \langle p \rangle - \alpha^- \langle -p \rangle) \underline{\mathbf{I}} \right) \quad (12)$$

and the scalar  $g$  is given by

$$g = \sqrt{3J_2(\underline{\mathbf{S}}) + \alpha^+ \langle p \rangle^2 + \alpha^- \langle -p \rangle^2}. \quad (13)$$

Polymeric materials are highly strain-rate dependent. A viscoplastic formulation is therefore used to take the strain rate effect on the yield surface into account. To include rate-dependent plasticity (viscoplasticity), an overstress [14] is defined in order to extend the (static) yield surface  $f$  (Eq. (7)). This extension implies that the yield surface is not only negative (i.e., elastic state) or null but can be positive (i.e., viscoplastic state). In the constitutive model, the overstress is defined by

$$\sigma^v = \left\langle \frac{(\eta - 1)I_1(\underline{\boldsymbol{\sigma}}) + \sqrt{(\eta - 1)^2 I_1^2(\underline{\boldsymbol{\sigma}}) + 12\eta J_2(\underline{\mathbf{S}})}}{2\eta(1 - D)} - \sigma_t - R(\kappa) \right\rangle. \quad (14)$$

$\sigma^v$  is the viscous stress which represents the difference between the static and the dynamic yield surface. Usually, in Perzyna-type viscoplastic model, the viscoplastic multiplier  $\dot{\lambda}$  is function of the overstress. In the constitutive model the viscoplastic multiplier is postulated such as

$$\dot{\lambda} = \frac{\eta^{vp}}{\sqrt{\frac{2}{3} \underline{\mathbf{n}} : \underline{\mathbf{n}}}} \left\langle \frac{\sigma^v}{\sigma_t + R(\kappa)} \right\rangle^{1/n}, \quad (15)$$

where  $n$  is the strain rate sensitivity parameter and  $\eta^{vp}$  is the viscosity parameter.

### 3 Nonlocal isotropic damage model

During the deformation of semi-crystalline polymers where mineral charges are introduced, the well-known cavitation phenomenon occurs. The cavitation is due to decohesion of the matrix-particles interface. In this case the viscoplastic deformation is accompanied by the damage process in the form of nucleation, growth and coalescence of cavities [15,16]. In the constitutive model, a phenomenological damage model is introduced in order to represent this cavitation. In this work, an isotropic damage, represented by a scalar variable  $D$  is therefore introduced in the constitutive equations. The nucleation and growth of micro-voids and micro-cracks during the deformation of filled polymer materials under tensile loading induce a softening behaviour. The finite element simulation of materials exhibiting strain softening leads to the well-known localisation phenomenon of the deformations in a narrow zone of the structure. This localisation phenomenon induces pathological dependency of the finite element mesh on the numerical responses. In order to overcome the spurious mesh dependency, an integral-type nonlocal model [10,11], where a damage variable defined by a spatial averaging, is used in the constitutive model. The nonlocal variable  $\bar{a}$  in a material point  $\vec{x}$  is mathematically defined as a weighted average of the local values  $a$  in all material points of the body  $B$ , such as

$$\bar{a} = \frac{1}{\psi(\vec{x})} \int_B \Psi(\vec{x}, \vec{y}) a(\vec{y}) dB(\vec{y}). \quad (16)$$

$\Psi(\vec{x}, \vec{y})$  is a Gaussian type weight function given by

$$\Psi(\vec{x}, \vec{y}) = \frac{1}{c} \exp\left(-\frac{r^2}{2l^2}\right), \quad (17)$$

where the scaling factor  $c$  depends on the problem dimension.  $c$  is defined by  $\sqrt{2\pi d}$  for one dimension,  $2\pi^2$  for two dimensions and  $\sqrt{\frac{\pi^3}{2}} l^3$  for the three dimensional case. The weight function depends only on the distance  $r = \|\vec{x} - \vec{y}\|$ . The intrinsic length  $l$  determines the size of the volume which effectively contributes to the nonlocal quantity. In the above integral, the local continuum viscoplasticity is retrieved if  $l$  tends towards zero. In order to have a nonlocal quantity equals to its corresponding local quantity  $a$  for homogeneous local values, the normalizing factor  $\psi(\vec{x})$  introduced in Eq. (16) is given by

$$\psi(\vec{x}) = \int_B \Psi(\vec{x}, \vec{y}) dB(\vec{y}). \quad (18)$$

The numerical implementation of an integral-type nonlocal model requires to have access to all the integration points of the finite element mesh in order to satisfy the consistency conditions of the material model in all the material points at the end of the time step. Unfortunately, in a user-material provided by most of commercial finite element codes, all the integration point information are not available at the same time. Furthermore, from the nonlocal nature of the problem, the resolution of constitutive equations becomes complex. An alternative nonlocal formulation proposed by Tvergaard and Needleman [17] is used in order to overcome these difficulties. The above authors have proposed a nonlocal version of the Gurson model where the local variable representing the void volume fraction

$\dot{f}$  is replaced by  $K^{nl} \dot{f}$ , where  $K^{nl} = \frac{\bar{f}}{f}$ . the penalty factor  $K^{nl}$  is therefore the ratio between a

local and a nonlocal quantity calculated at the previous time step. With this nonlocal formulation, the above authors have noted that the mesh sensitivity have been completely removed for a sufficiently fine mesh relative to the material intrinsic length. Following the above concept, a nonlocal factor  $K^{nl}$  is introduced in the damage evolution in order to take the damage values of the averaging elements into account. The quantity  $K^{nl}$  is also computed by

$$\mathbf{K}^{nl} = \frac{\overline{\dot{D}_n}}{\dot{D}_n}, \quad (19)$$

where  $\overline{\dot{D}_n}$  is the nonlocal damage rate calculated with the averaging operator from the local damage rate  $\dot{D}_n$  arising from the previous time step. With this formulation, only the scalar  $\mathbf{K}^{nl}$  is introduced in the constitutive equations and the local form of the constitutive equations is therefore conserved. In the constitutive model, the evolution of the damage variable is postulated following

$$\dot{D} = \frac{\dot{\lambda}}{g(1-D)} \sqrt{3J_2(\underline{\mathbf{S}}) + \frac{2}{9}(\alpha^+ \langle p \rangle + \alpha^- \langle -p \rangle)^2} \exp\left(\frac{-\kappa}{k_c}\right), \quad (20)$$

where  $k_c$  is a material parameter.

This constitutive model is implemented in Fortran 90 in a user-material subroutine for the explicit finite element software LS-DYNA®. An implicit scheme is used for the stress update and the viscoelastic predictor/viscoplastic corrector scheme is used to solve the constitutive equations. In order to implement the nonlocal procedure, since a Lagrangian regularisation is assumed, a nonlocal averaging operator is computed only at the first time step and the nonlocal factor  $\mathbf{K}^{nl}$  is computed at each time step from the previous value of the damage rate. The details of the implementation of the constitutive model and the procedure for the identification of the material parameters are given in [18].

## 4 Numerical results

Numerical results in term of mesh dependency on a three-dimensional cylindrical bar meshed with solid elements are firstly presented. The simulations are performed on a mineral filled semi-crystalline polymer (polypropylene) used in automotive application exhibiting strain softening due to the cavitation involved in the viscoplastic deformation process. A comparison between the numerical model and experiments are presented at the end of this section.

### 4.1 Three dimensional necking bar analysis

The mesh independence of the constitutive model is verified on the necking simulation of a three-dimensional cylindrical bar in tension. The cylindrical bar with a length of 53.334 mm and a radius of 12.826 mm is subjected to uniaxial tension up to a total axial elongation of 8 mm (with a velocity of 1 mm/s). For symmetry reasons, the analysis is performed on the eighth of the geometry with the appropriate boundary conditions. In order to evaluate the mesh sensitivity of the constitutive model, three different meshes with 663, 2100 and 6300 reduced integrated eight node hexahedral elements are simulated with and without the nonlocal damage regularization<sup>3</sup>. The three different meshes are shown in Fig. 1. The three meshes contain a geometric imperfection of 1.8 % at the bottom in order to trig the necking in the centre of the cylindrical bar. For the following and for all the simulations carried out in this section, the material parameters used are given by [18].

<sup>3</sup> The local damage model is recovered by setting the nonlocal factor  $\mathbf{K}^{nl}$  to 1 for all the gauss points.

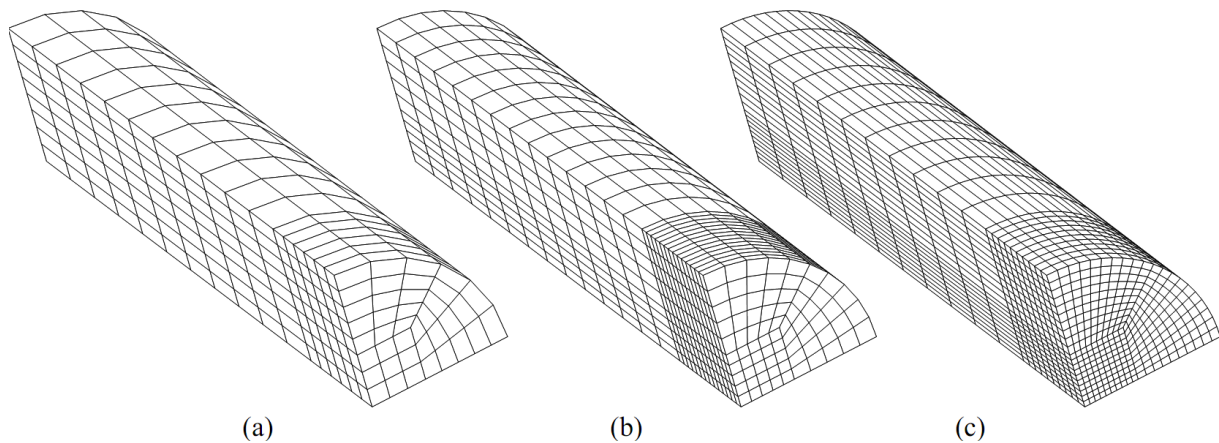


Fig. 1: Three-dimensional cylindrical bar necking. Finite element meshes of 663 (a), 2100 (b) and 6300 (c) elements.

An intrinsic length of 1 mm is used for the nonlocal regularisation. The deformed shapes resulting to the simulations of the three meshes without the nonlocal regularisation is shown in Fig. 2. For the three meshes simulated with the local model, larger deformations of the elements in the center of the bar are observed. A localisation of the deformations in the elements where the necking occurs takes place.

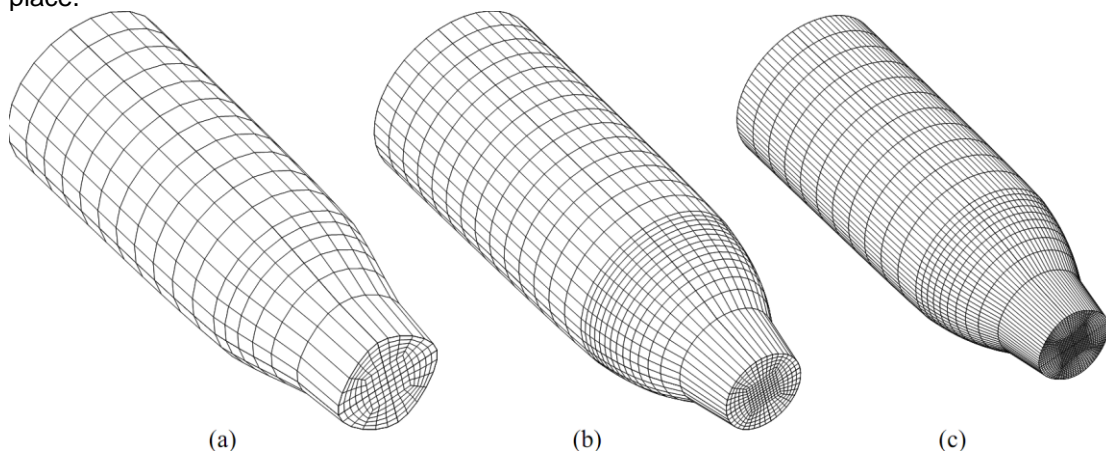


Fig. 2: Three-dimensional cylindrical bar necking. Deformed shapes for the three meshes with 663 (a), 2100 (b) and 6300 (c) elements simulated without the nonlocal regularisation.

Fig. 3 shows the deformed shapes for the three meshes simulated with the nonlocal model.

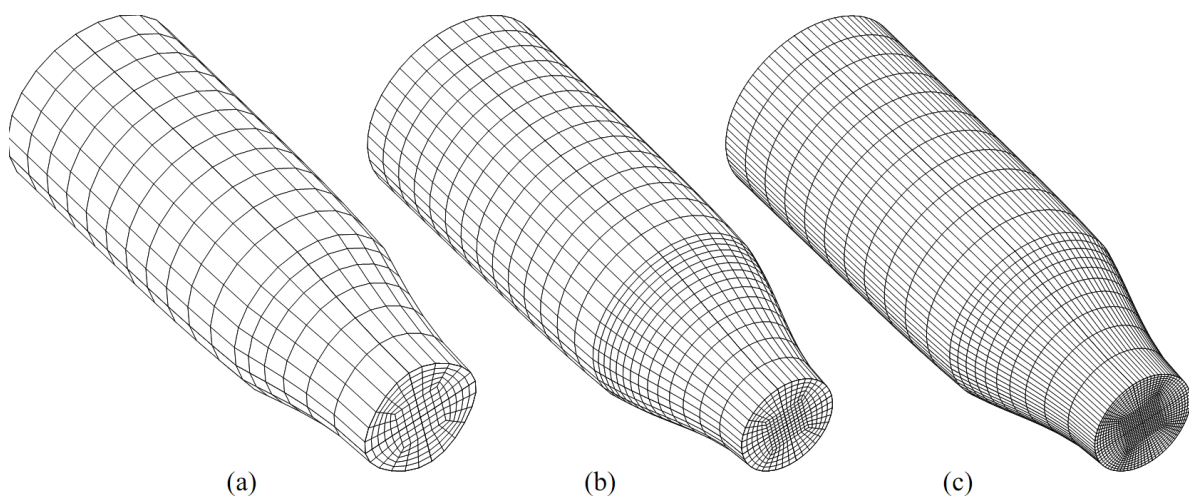


Fig. 3: Three-dimensional cylindrical bar necking. Deformed shapes for the three meshes with 663 (a), 2100 (b) and 6300 (c) elements simulated with the nonlocal regularisation.

The spurious localisation of the deformation in the elements at the necking does not occur. The deformations of the elements in the centre of the bar are not over-estimated in comparison with the around elements. The reaction forces at the bottom of the meshes versus the displacements at the top boundaries for the six simulations are shown in Fig. 4.

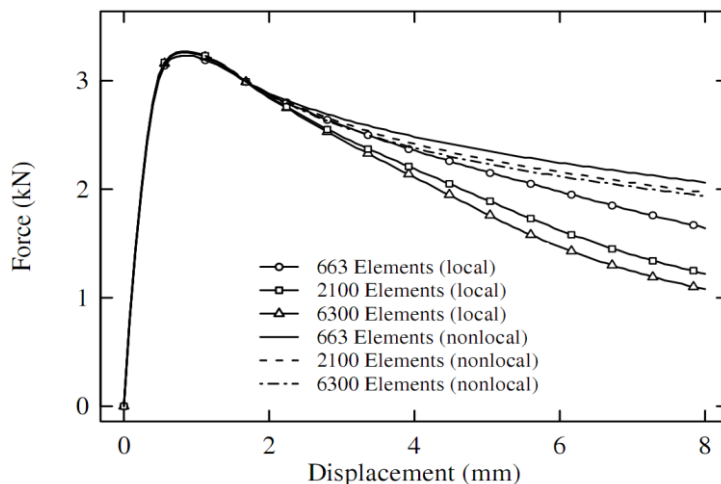


Fig. 4: Force response of the simulations for the 3 different meshes and the two damage models (local and nonlocal).

The simulations carried out with the local damage model have the same results in term of force-displacement until an axial elongation of 2mm. For a more important elongation, the responses of these simulations become mesh dependent. By using the nonlocal formulation of the damage model, the responses of the simulations are very close. The nonlocal damage averaging play its rule of localisation limiter and the results becomes mesh independent.

#### 4.2 Comparison with experiments

The numerical uniaxial tensile tests presented in this section are carried out for the 5 following loading speeds: 1, 100 mm/min, 0.08, 0.8 and 4 m/s. The geometry of the specimen, boundary conditions and finite element mesh are shown in Fig. 5. For the simulations, the specimen is meshed with reduced integrated shell elements and 3 integration points through the thickness are used. The loading consists on a prescribed monotonic velocity (with free horizontal displacement) on the nodes of the right edge of the mesh. The comparisons between the constitutive model and the experimental data are shown in Fig. 6. The reaction forces at the left of the specimens versus the displacements enforced at the right boundaries are compared with the experimental data. The constitutive model results are in agreement with the experimental measurements for all the speed loadings. In order to show the accuracy of the viscoelastic model, Fig. 7 shows the comparison between the numerical model and the experimental data for three speed loadings: 1, 50 mm/min and 0.08 m/s. The results are focused on the first part of the curves where the viscoelastic part can be visualised easily. The numerical model has a good prediction of the stiffness of the material loaded at various speed loadings. In order to compare the evolution of the local logarithmic strains (longitudinal and transverse) of the numerical model with the experimental observations, Fig. 8 shows the true stresses (Cauchy)-strains (Henky) responses of one element in length gauge of the specimen given by the numerical model with the experimental measurement (by DIC) for 4 different speed loadings. The longitudinal and transverse logarithmic strain components are well captured by the non-associative viscoplastic constitutive model.

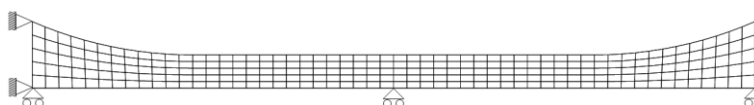


Fig. 5: Finite element mesh and boundary conditions of the tensile specimen.

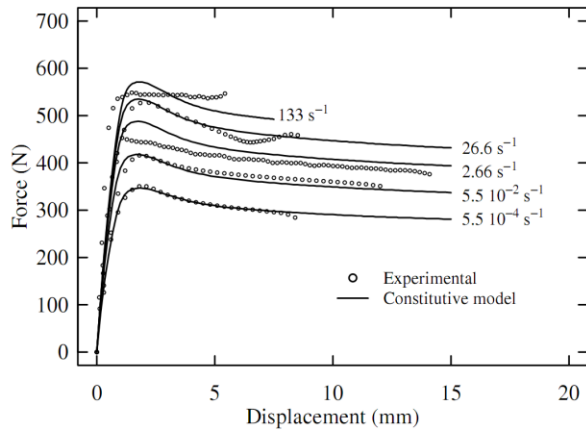


Fig. 6: Experimental vs. constitutive model in uniaxial tensile loading.

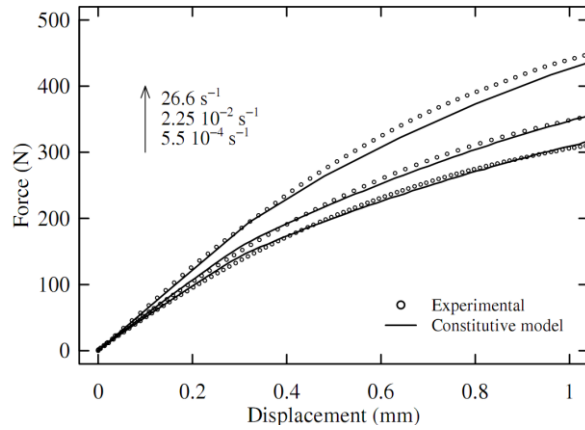


Fig. 7: Experimental vs. constitutive model in uniaxial tensile loading.

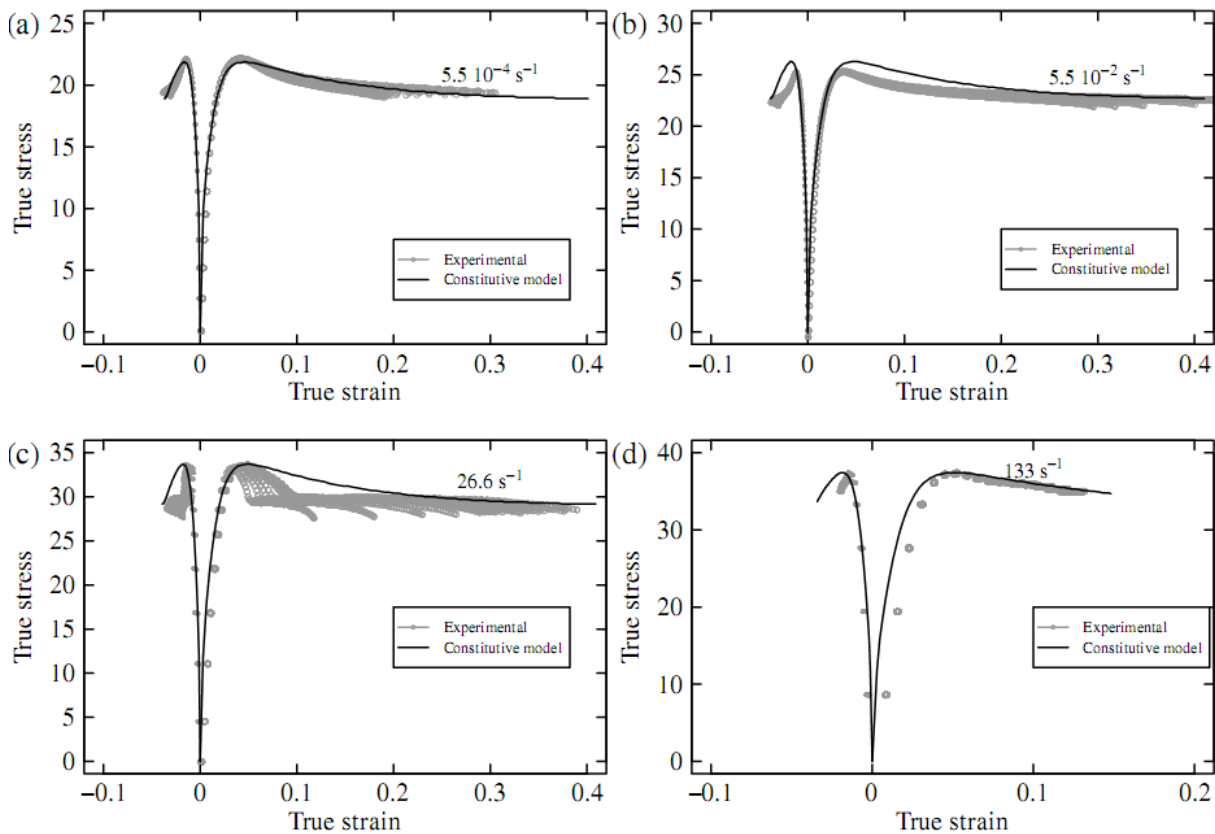


Fig. 8: Experimental vs. constitutive model in uniaxial tensile loading.

## 5 Acknowledgements

The present research work has been supported by the International Campus on Safety and Intermodality in Transportation, the Nord-Pas-de-Calais Region, the European Community, the Regional Delegation for Research and Technology, the Ministry of Higher Education and Research, and the National Center for Scientific Research and TOYOTA MOTOR EUROPE.

## 6 References

- [1] Boyce, M.C., Parks, D.M., Argon, A.S., "Large inelastic deformation of glassy polymers. part I: rate dependent constitutive model". *Mechanics of Materials* 7, 1988, 15-33.
- [2] Arruda, E.M., Boyce, M.C., "A three-dimensional constitutive model for the large stretch behavior of rubber elastic materials". *Journal of the Mechanics and Physics of Solids* 41, 1993, 389-412.
- [3] Krempl, E., McMahon, J., Yao, D., "Viscoplasticity based on overstress with a differential growth law for the equilibrium stress". *Mechanics of Materials* 5, 1986, 35-48.
- [4] Ho, K., Krempl, E., "Extension of the viscoplasticity theory based on overstress (vbo) to capture non-standard rate dependence in solids". *International Journal of Plasticity* 18, 2002, 851-872.
- [5] Krempl, E., Khan, F., "Rate (time)-dependent deformation behavior: an overview of some properties of metals and solid polymers". *International Journal of Plasticity* 19, 2003, 1069-1095.
- [6] Steenbrink, A.C., Giessen, E.V.D., Wu, P.D., "Void growth in glassy polymers". *Journal of the Mechanics and Physics of Solids* 45, 1997, 405-437.
- [7] Voyiadjis, G.Z., Shojaei, A., Li, G., "A generalized coupled viscoplastic-viscodamage-viscohealing theory for glassy polymers". *International Journal of Plasticity* 28, 1992, 21-45.
- [8] R. Balieu, F. Lauro, B. Bennani. "Modèles de comportement pour matériaux polymères soumis au crash", 2011, 10ème colloque national en calcul des structures, hal.archives-ouvertes.fr.
- [9] Hiermaier, S., Balieu, R., Lauro, F., Bennani, B., Bourel, B., Nakaya, K., "Polymer behaviour and fracture models in dynamic", *EPJ Web of Conferences*, 2012.
- [10] Bažant ZP, Lin FB., "Non-local yield limit degradation". *International journal for numerical method in engineering*, 26(5), 1988, 05–23.
- [11] Jirásek M, Rolshoven S. "Comparison of integral-type nonlocal plasticity models for strain-softening materials". *International Journal of Engineering Science*, 41, 2003, 553-602.
- [12] Xiao, H., Bruhns, O.T., Meyers, A., "Logarithmic strain, logarithmic spin and logarithmic rate". *Acta Mechanica* 124, 1997, 89–105
- [13] Raghava, R., Caddell, R.M., Yeh, G.S.Y., "The macroscopic yield behaviour of polymers". *Journal of Materials Science* 8, 1973, 225-232.
- [14] Perzyna, P., "Fundamental problems in viscoplasticity". *Advances in Applied Mechanics* 9, 1966, 243-377.
- [15] Gurson, A.L., "Continuum theory of ductile rupture by void nucleation and growth, 1. Yield criteria and flow rules for porous ductile media". *Journal of Engineering Materials and Technology-Transactions of the ASME*, 1977, 2-15.
- [16] Croix, P., Lauro, F., Oudin, J., Christlein, J., "Improvement of damage prediction by anisotropy of microvoids". *Journal of Materials Processing Technology*, 2003, 202-208.
- [17] Tvergaard V, Needleman A. "Effects of nonlocal damage in porous plastic solids". *International Journal of Solids and Structures*, 1995, 63-77.
- [18] Balieu R. A fully coupled viscoelastic-viscoplastic damage model for semi-cristalline polymers. Ph.D. thesis, 2012, Univ. Valenciennes.